



Blending and emission characteristics of biogasoline produced using CaO/SBA-15 catalyst by cracking used cooking oil

Shengbo Ge^a, Ramya Ganesan^b, Manigandan Sekar^c, Changlei Xia^{a,*}, Sabarathinam Shanmugam^d, Mishal Alsehli^e, Kathirvel Brindhadevi^{f,g,*}

^a Co-Innovation Center of Efficient Processing and Utilization of Forestry Resources, College of Materials Science and Engineering, Nanjing Forestry University, Nanjing, Jiangsu 210037, China

^b Department of Chemistry, St. Joseph's Institute of Technology, Chennai 600 119, India

^c Department of Aeronautical Engineering, Sathyabama Institute of Science and Technology, Chennai, India

^d Department of Microbial Biotechnology, Bharathiar University, Coimbatore, Tamil Nadu 641046, India

^e Mechanical Engineering Department, College of Engineering, Taif University, P.O. Box 11099, Taif 21944, Saudi Arabia

^f Department of Pharmacology, Saveetha Dental College, Saveetha Institute of Medical and Technical Sciences, Saveetha University, Chennai, India

^g Faculty of Electrical and Electronics Engineering, Ton Duc Thang University, Ho Chi Minh City, Viet Nam

ARTICLE INFO

Keywords:

Biofuels
Used cooking oil
Torque
Fuel consumption
CO, SO₂

ABSTRACT

The aim of this work is to crack the used cooking oil in a fixed bed cracking unit using impregnated CaO/SBA-15 catalyst to yield liquid hydrocarbons with high % of biogasoline (BioG) fraction. Further, to investigate the capacity of the biogasoline fraction as well as the bio gasoline blends with fossil gasoline in increasing its efficiency. The porous morphology, pore distribution and surface area, elemental composition and phase formation of catalysts were analysed by Scanning electron Microscopy, Surface area analyser and X-ray diffraction techniques. All the synthesized materials were crystalline and least changes were observed with incorporation of CaO on SBA-15. The morphology of the materials were as expected without much agglomeration. SBA-15 exhibited fair surface area of around 1300 m²/g and discrete pores gas chromatography mass spectrometry (GC-MS). Among the catalysts, the composite material, CaO/SBA-15 (4 wt%) efficiently cracked 97% of used cooking oil into 70% liquid products and 69.7% of biogasoline which was confirmed using gas chromatography-mass spectrometry (GC-MS). BioG showed a good Calorific value of 10000 MJ/Kg which was comparable to that of petroleum fuel. Results of the engine test indicated that using biogasoline-gasoline blended fuels, torque output and fuel consumption of the engine increased when compared to gasoline; CO and SO₂ emissions decreased largely due to the oxidation, CO₂ emission increased because of the improved combustion and NO_x emission from bio gasoline blends was low than gasoline.

1. Introduction

Biofuel is the right solution to the crisis the world is facing at present. Today we face energy scarcity, spike in petroleum prices, threatening pollution and steering temperature [1,2]. The doorway to such issues is figuring out a prompt choice that can deliver an efficient fuel which is renewable, biodegradable and environmentally benign, and compatible to an existing engine [3,4]. Biomass has always existed as a prominent source for deriving biofuels, however; the existence of controversy over food over fuel restricted their exploration. The consideration of edible oil crops (peanut, sunflower, palm, sugarcane) was forbidden within a

few years of research due to their low availability and critics [5,6]. Non-edible oil crops and seeds are sought to be the better options compared to the former as they are abundantly available for they are not considered as food. Extending the work has lead to focus on used cooking oil which can be overlooked as an economic and green option [7,8]. It is wise to derive energy from them as consumption of such oils will lead to health hazards too. Several works are reported on the biofuel production using used cooking oil namely palm, sunflower, [9], rice bran [10], etc. India, the country known for its deep-fried foods, has to tackle the large production of used oil and this approach can be of timely help. The wide range of biofuels is biohydrogen, biogas (gaseous fuels), bioethanol,

Abbreviations: UCO, Used cooking oil; SBA-15, Santa Barbara Amorphous-15; MCM-41, Mobil Composition of Matter No. 41; BioG, Biogasoline.

* Corresponding authors.

E-mail addresses: changlei.xia@njfu.edu.cn (C. Xia), kbrindha19@gmail.com (K. Brindhadevi).

<https://doi.org/10.1016/j.fuel.2021.121861>

Received 22 July 2021; Received in revised form 17 August 2021; Accepted 27 August 2021

Available online 6 September 2021

0016-2361/© 2021 Elsevier Ltd. All rights reserved.

biopropanal, biodiesel, organic liquid hydrocarbons (liquid fuels), and biochar (solid fuel) [11–13]. The drastic increase in motor vehicles in every part of the world demands petroleum fuel in large quantities. The handful of techniques and methodologies available to process the oil or triglycerides into biofuels makes the appropriate selection quite simple. Complete gasification of biomass and consequent condensation to form liquid fractions is known as pyrolysis [14]. The fuel obtained from pyrolysis is referred as bio oil, rich in oxygenated compounds. Ahmed et al. [15] and Fu et al. [16] reported low calorific value of biooil and however, other properties such as flash and fire point were in agreement with ASTM and EN standards. Reports are in scarce that emphasize the use of Bio oil as such in engine. Prasad and Murugavel, [17] have tried blending biooil with commercial petroleum and proposed a 10–12% blend has remarkable action. Transesterification, the most common technique that converts the vegetable oil or animal fats into C-18 fatty acid esters (biodiesel) are also one of the better competitors in the production of biofuel. Biodiesel, built of esters, is not advisable for direct usage in the present day engines as it leads to choking and failure of the engine. The expectation of using the fuel directly into engine without further blend makes catalytic cracking process a good choice as the lower working temperature in this process compared to pyrolysis elevates the ease of work and energy efficiency [18,19]. Breaking a long chain of fatty acid of oil vapours into shorter chain with lower oxygen contents and that exactly replicates the fossils is only possible from Catalytic Cracking process. The products of cracking reaction include liquid hydrocarbons (C5 - C18 range) and gas (<C5; more % of propane and butane). Fixed bed catalytic cracking technique in cracking of oil to produce biofuel was proposed by Zhang et al. [20] in cracking non edible oils using sulphated TiO₂/ZrO₂ catalyst and Ganesan et al. [21] for producing Organic liquid hydrocarbons from castor and mustard oil by cracking over H_β and AlMCM-41 materials. Non-edible vegetable oils namely *jatropha curcus*, *Millettia pinnata*, *Azadirachta indica*, palm kernels and used cooking oil were cracked in presence of catalyst and reported with higher percentage of lower hydrocarbons [21–23]. Catalytic cracking reaction is believed to follow the carbonium ion theory that comprises of initiation, followed by propagation and termination. Cracking of vapours would require a special feature in catalyst that provides cavity of proper diameter and channelling with moderate acidity [24]. Na₂CO₃, CaO and K₂CO₃ have been reported to crack palm and soya bean oil to produce biofuel [25,26]. Interestingly, extreme catalytic activity was showed by basic metal oxide; CaO in producing biodiesel by transesterification process as well as in cracking of oil [27,28]. CaO is known to reduce the acid value and rupture the rings to reduce the aromatic content. The activity of CaO catalyst was studied by Pradana et al. [29] in cracking sugarcane bagasse into liquid fuels. Cracking ability of calcium oxide catalyst on rice hull was reported by Gan et al. [30]. Ni/Ca-Fe catalyst was employed in pyrolysis of biomass to produce bioliquid hydrocarbons by Lu et al. [31]. Nevertheless, it delivers higher percentage of oxygenated compounds as it hinders the pyrolysis of esters [32]. Whereas, solid acid catalysed reactions produced liquid with low oxygen content and less viscosity. A hybrid of porous and oxide catalysts should bestow porous sites with acidic nature. Porous materials with pore diameter from 2 nm to 100 nm, such as, β, Zeolite Socony Mobil-5 (ZSM-5), Y, Mordenite Zeolites (MOR), MCM-n, SBA-n are examined for their catalytic activity in cracking vegetable oils [33,34]. SBA-15 is a mesopore with pore diameter of 5 to 15 nm has uniform hexagonal pores and narrow pore size distribution. Attractive properties of SBA-15 that makes it a perfect choice for the current study are a) high surface area (500–1500 m²/g), b) credible thermal and mechanical stability, c) more tolerant and poses less threat to the environment [35]. SBA-15 is a mesoporous silica material with well organised nanopores and a large surface area that is used as catalyst supports, absorbents, drug delivery materials, and other applications. Heteratoms and organic functional groups have been introduced by direct or post-synthesis methods to enhance its functionality due to its lack of usefulness. However, the material is barely siliceous and acidic

nature can be incorporated by introducing hetero atom, ex. Al³⁺ and Zr³⁺ into the tetrahedral lattice. Significant increase in selective product yield was attained by using AlMCM-41, AlMCM-48 and AlSBA-15 in cracking Zhang et al. [36] and Xu et al. [37]. This work is the first attempt to understand the activity of basic oxide loaded mesoporous material CaO/SBA-15.

Standards of alternative fuel set by ASTM standards includes the physical parameters and exhaust emissions from engine. Engine studies and emission analysis of the biofuel were investigated and reported by Mangesh et al. [38], Ashour et al. [39] and Dinesha et al. [40]. In this present work, the properties of liquid biofuels were analyzed as per ASTM standards and engine was operated with B100, B75, B50, B25 and B5 blends. The results are discussed herein.

2. Materials and methods

2.1. Materials required

Tetra ethyl ortho silicate (TEOS) used as silicon source was procured from SRL, India. Pluronic P123 and Calcium acetate was purchased from Chemplast, India. The raw source required for production of fuel was procured from our college kitchen. The frequent cooking of deep fried food stuffs provided ample used cooking oil. This is generally regarded as waste and neglected for further use.

2.2. Synthesis of SBA-15

Procedure proposed by Adrover et al. [41] was followed for the synthesis of the cubical SBA-15 material. The composition of the obtained gel was: 0.5 TEOS: 0.0085 P123: 2.84 HCl: 98.5 H₂O. The non-ionic tri-block copolymer, Pluronic P123 (EO20PO70O20) was dissolved in hydrochloric solution in a 250 mL polypropylene beaker at 40 °C. The surface directing agent, TEOS was slowly introduced into the medium maintained at 40 °C under continuous stirring for 2 h. The hydrothermal synthesis of catalyst was performed at 100 °C for 24 h in a hot air oven in a sealed polypropylene bottle. Filtration of the product mixture using Büchner filter followed by washing with distilled water and overnight drying resulted in solid mass. The solid mass was calcined in a muffle furnace at 350 °C under air for 3 h with a heating rate of 1 °C/min.

2.2.1. Wet impregnation of Calcium ions onto the SBA-15

SBA-15, the mesoporous material was loaded with Ca²⁺ ions by wet impregnation technique. About 75 mL of 0.1 M solution of Calcium acetate was added to 2 g of the synthesized SBA-15 catalyst. The mixture was stirred using hot pad magnetic stirrer for 2 h at 60 °C. The resultant solution was filtered and the obtained solid material was washed thoroughly with distilled water and dried at room temperature. Different loading of Ca²⁺ (2 to 10 wt%) on SBA-15 were synthesized and used for cracking reactions.

2.3. Catalytic cracking of UCO

UCO was catalytically upgraded to deliver fuels with improved characteristics using the synthesized CaO/SBA-15 catalyst (Fig. 1). Weight Hourly Space Velocity (WHSV) of 4.6 h⁻¹ was fixed for cracking UCO. Our previous works has reported a significant % of gasoline delivered at WHSV of 4.6 h⁻¹ and the present work was performed at same WHSV [42]. About 0.5 g of catalyst was packed in the middle of a quartz reactor of 2 cm id and 40 cm length dimension. The reactor was placed in a tubular furnace which was electrically heated up to 450 °C. The products were condensed using chiller unit and the liquid and gaseous products were collected separately. GC-MS (GC-MS, Agilent HP 6890 models 19091S-433, HP-5MS capillary column 30 m × 250 μm × 0.25 μm) analysis was performed to analyse the liquid and gas fragments of composition of cracked oil. N-Heptane was used as the standard for

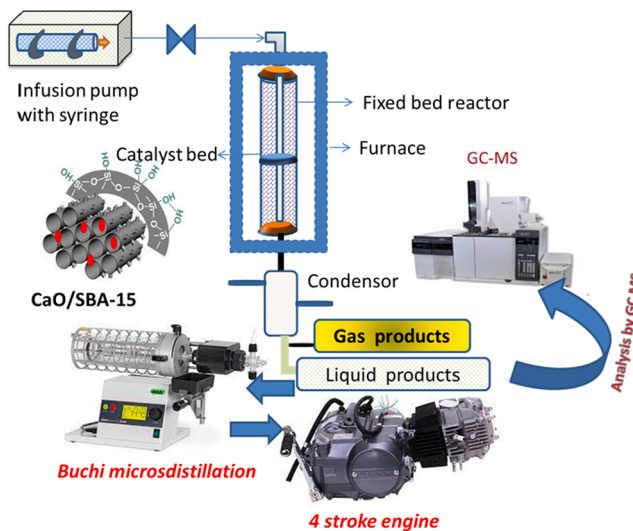


Fig. 1. Reactor setup of fixedbed catalytic cracking unit.

validating the presence of gasoline in the BioG. The authentic hydrocarbons' retention time was compared to the retention time of the hydrocarbons in the sample. By injecting comparable commercial samples of gasoline, kerosene, and diesel into a gas chromatograph, the retention durations for each fraction were determined. According to their boiling ranges, the Biofuel is divided into three fractions: GG fraction (60–120 °C), GK fraction (120–180 °C), and GD fraction (180–250 °C). The equation used for calculating the % conversion and % of Gasoline present in liquid product is:

$$\text{Conversion (\%)} = \frac{\text{Sum of Liquid Fuel (g), Gas(g)and Water(g)}}{\text{Mass of the Feed}} \quad (1)$$

% Yield of Liquid Fuel and gaseous hydrocarbons

$$= \frac{\text{Mass of Liquid Fuel (g)or mass of gas (g)}}{\text{Mass of the Feed}} \quad (2)$$

$$\% \text{ of fraction} = \frac{\text{Mass of Bio G or Bio K or Bio D fraction (g)}}{\text{Mass of Liquid Fuel (g)}} \quad (3)$$

The obtained liquid products were separated using BUCHI Micro Distillation unit (BUCHI K – 350).

2.4. Catalyst characterization and product analysis

Elemental analysis was investigated by the Energy Dispersive X-ray (EDX) technique using VEGA//BSE (Backscattered electron) detector. The phase formation was confirmed by Powder XRD patterns recorded using Cu KR radiation of wavelength 1.54060 Å° on PANalytical Xpert PRO X-ray diffractometer. Measurements were carried out at 20 angles from 1.5° to 5°. Autosorb- iQ-MP/XR volumetric adsorption analyser measured the surface area of the material at liquid N₂ temperature by using 30:70 ratio (N₂: He). Before the measurements, the sample was degassed under flow of N₂ at 200 °C for 2 h. JEOL JSM-6360 scanning electron microscope operated 20–30 kV scanned the morphology of the material. Bruker EQUINOX 55 Model FTIR analysed biooil and BioG was recorded in the transmission mode between 4000 cm⁻¹ and 400 cm⁻¹ with dried KBr pellets.

2.5. Engine specifications

The engine used for the study is a gasoline run engine that is air cooled, 4 S, single cylinder OHC and direct injection. The engine's specification is given in Table 1. An eddy current dynamometer was used to measure load and engine speed. The engine was designed to measure

Table 1
Specifications of engine used for studies.

Type of engine	4 cylinder
Displacement	149.2 cc
Bore X stroke	57.3 × 57.8 mm
Maximum Torque	12.80 N m @ 6500 rpm
Compression ratio	9.1:1
Cooling system	Air cooled
Maximum power	10.6 KW (14.4 Ps) @8500 rpm
Acceleration	0–60 kmph in 5 sec
Maximum speed	107 kmph

fuel consumption, engine speed and exhaust gas temperature. The engine fluctuation was avoided by warming the engine for 5 to 7 min. Engine was tested at full load condition by varying the speed of engine from 1000 to 3000 rpm and, blends of BioG were tested for reproducibility and the observations of exhaust emissions and engine performance are reported in this study. At a constant operating condition, the fuel was injected into the engine through a nozzle fuel injection port. The volume of blend was controlled by engine control unit which injected BioG at a specific voltage. A typical fuel injector system was connected to the pump to which engine control unit was also plugged. The values were recorded after the engine reached its stable condition. Pure commercial gasoline and different blends of BioG (B10, B230, B50 and B70) were used to operate the engine. A constant speed of 1500 rpm was maintained and the parameters considered as significant for performance were studied. Extrel Residual gas analyser was used to study the exhaust gas emission (NO, CO₂, CO and Hydrocarbon) from the engine.

3. Results and discussion

3.1. Characterization

Fig. 2a illustrates the EDX results of synthesized CaO/SBA-15 nanocatalysts. This analysis was performed to determine the dispersion of the loaded element over the catalysts. The figure shows the Ca, O, Si, and Ca elements in the nanocatalysts structure. Similar results were also observed by Dehghani and Haghghi [43]. The purity of the catalyst can be confirmed by the absence of any unrecognized indicator peak in the spectrum. Three intense peaks are seen in the powder XRD pattern of SBA-15 (**Fig. 2b**) which is a basic characteristic of any hexagonally ordered material. The peaks were indexed at [100], [110] and [200] reflections related to the peaks between the angle of 1.2 and 2.5. Shi et al. [44] reported the same diffraction peaks for the synthesized mesoporous SBA-15 material. However, the CaO impregnated SBA-15 showed slightly distorted peaks shifted to higher angles. The increase in loading of Ca²⁺ ions on SBA-15 from 2 to 10 wt%, resulted in low intense peaks and peaks shifted to higher angle order. Li et al. [45] synthesized ZrO₂/SBA-15 and observed the shift in peak position with the loading of ZrO₂ molecules. However, the lattice structure was preserved and there is no phase distortion. Similar pattern were reported in the XRDs of mesoporous material such as MCM-41 and SBA-15 impregnated with other elements [46]. The change in the interspace lattice of the host (mesoporous) material would have contributed to the observation. The introduction of new atoms into lattice decreases the pore wall thickness which subsequently reduces the peak intensity. Surface area of SBA-15 was measured to be 1300 m²/g which was relevant to mentioned reports [47]. With increase in Ca²⁺ in the material, the surface area showed little drop; due to the Calcium ions occupancy on the surface. CaO/SBA-15 (2 wt%) had the maximum surface area (970 m²/g) and CaO/SBA-15 (10 wt%) had the lowest (890 m²/g). Surface area of the materials dropped with increasing % of CaO into the lattice. Verma et al. [48] also studied the impact of loading on SBA-15 material and observed the similar pattern. Adsorption isotherm of the synthesized material is shown in **Fig. 3a** which corresponds to type IV

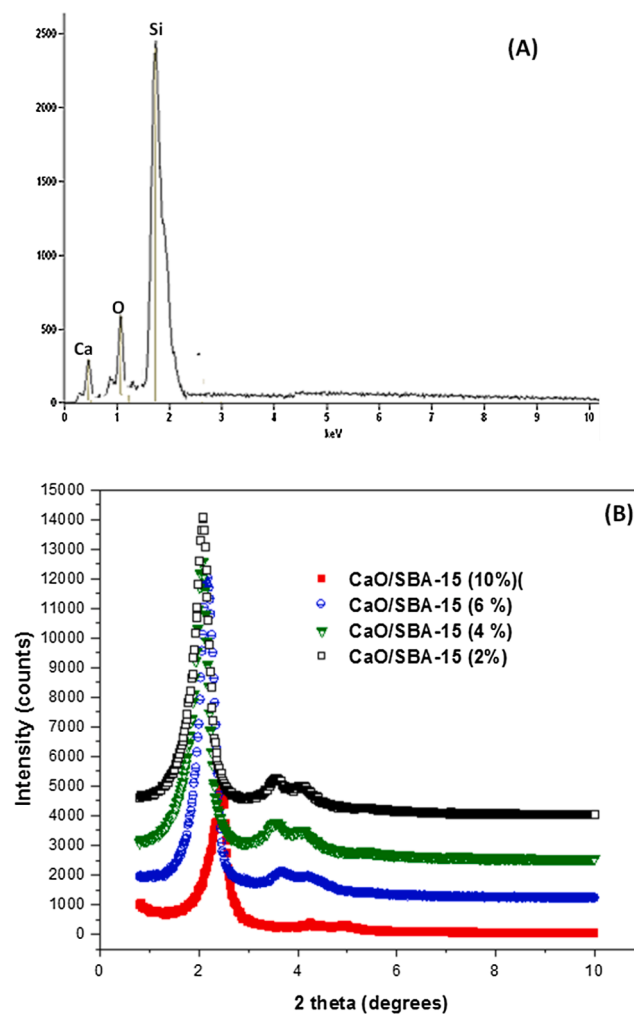


Fig. 2. EDX spectrum of CaO/SBA-15 (4 wt%) b) XRD spectrum of CaO/SBA-15 (2%, 4 wt%, 6 wt%, 8 wt% and 10 wt%).

isotherm. Mesoporous nature of a material is confirmed by this isotherm model and in addition, the H1 type of hysteresis seen in the curve is a characteristic of cylindrical pores of uniform pore size. The material has pores of size < 15 nm as shown in Fig. 3b. Thahir et al. [49] reports suggest the similar type IV adsorption isotherm pattern exhibited by this material. Fig. 4a illustrates the spherical morphological and structural features of the prepared catalyst in the FESEM study. It is clearly seen, that the lumped unloaded SBA-15 (Fig. 4a) is divided into smaller

particles by increasing the Ca^{2+} content (Fig. 4b). This observation matches with the XRD patterns that affirmed the increasing Ca^{2+} content decreased SBA-15 crystallinity.

3.2. Cracking ability of CaO , SBA-15 and $\text{CaO}/\text{SBA-15}$ materials on UCO

The catalytic efficiency of CaO , SBA-15 and different % of $\text{CaO}/\text{SBA-15}$ were investigated and the observation is shown in Fig. 5a and 5b. Both liquid and gaseous products are obtained from both the methods, but, there is significant difference in the % yield of products and selectivity of gasoline range of hydrocarbons. It was observed that $\text{CaO}/\text{SBA-15}$ showed a better result to their parent material; SBA-15 and CaO . $\text{CaO}/\text{SBA-15}$ increased the liquid yield but reduced the gas and coke yield while CaO showed the opposite trend. Basic oxide CaO converted 44% of oil into 27% of liquid product with 24% BioG fraction. SBA-15 cracked 63 % of UCO into 41% of liquid fuel with 30.4% of BioG. A sharp increase in product yield is observed while using the composite $\text{CaO}/\text{SBA-15}$ catalyst compared to bare CaO and SBA-15 catalysts. $\text{CaO}/\text{SBA-15}$ (2%) converted 94% of UCO into 66% of liquid fuel and with further increase in loading (4%), the conversion % increase to 97%. However, the consequent increase in loading of CaO on SBA-15 dropped the conversion to 86% with 70% liquid hydrocarbon. De Sousa Castro et al. [50] investigated the cracking of palm oil using yet another mesoporous material, AlMCM-41 impregnated with nickel. Similar trend in conversion was reported supporting the present investigation. In terms of gasoline selectivity, $\text{CaO}/\text{SBA-15}$ materials showed excellence compared to CaO and SBA-15. About 61% of gasoline selectivity was achieved using $\text{CaO}/\text{SBA-15}$ (2%) and a maximum of 70% was attained using $\text{CaO}/\text{SBA-15}$ (4 %). BioG % gradually decreased with more loadings of CaO on SBA-15. A study conducted by Cao et al. [35] used $\text{ZnO}/\text{SBA-15}$ to crack waste cooking oil produced 37.3% of biofuels which was lower than the obtained results.

3.2.1. GC MS analysis BioG obtained from UCO

Fig. 6 shows the GCMS analysis result of BioG obtained from UCO. GC MS plot of n-Heptane is given for comparison purpose. Manico et al. [51] reported the GC MS analysis of liquid fuel by comparing n-heptane for the presence of gasoline fraction. BioG is found to be relatively similar to n-Heptane. The peak at the lower retention period has a higher intensity than the peaks at the later retention durations. This shows the existence of higher levels of lower range hydrocarbons (C4 to C9), i.e. gasoline range hydrocarbons (75%) in the lower range [52]. Higher % of diesel range hydrocarbons was reported while cracking the palm oil with Ni/AlMCM-41 catalyst by de Sousa et al. [50].

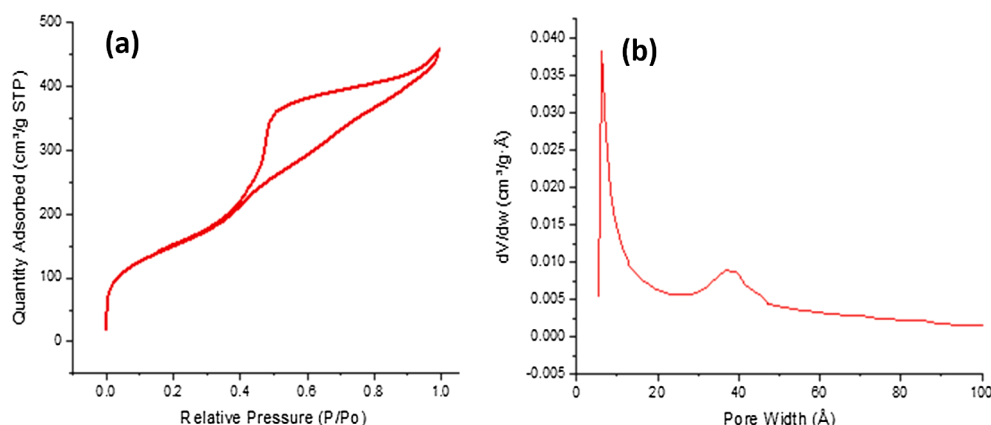


Fig. 3. a) Adsorption desorption isotherm of CaO/SBA-15 (4 wt%) b) pore size distribution of CaO/SBA-15 (4 wt%).

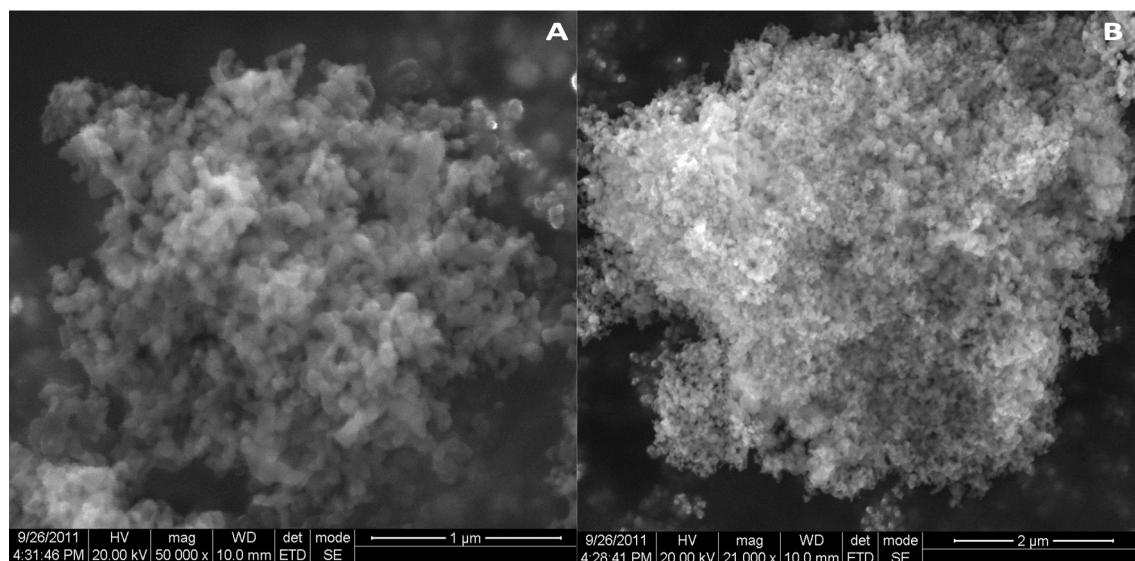


Fig. 4. FESEM image of a) SBA-15b) CaO/SBA-15 (4 wt%).

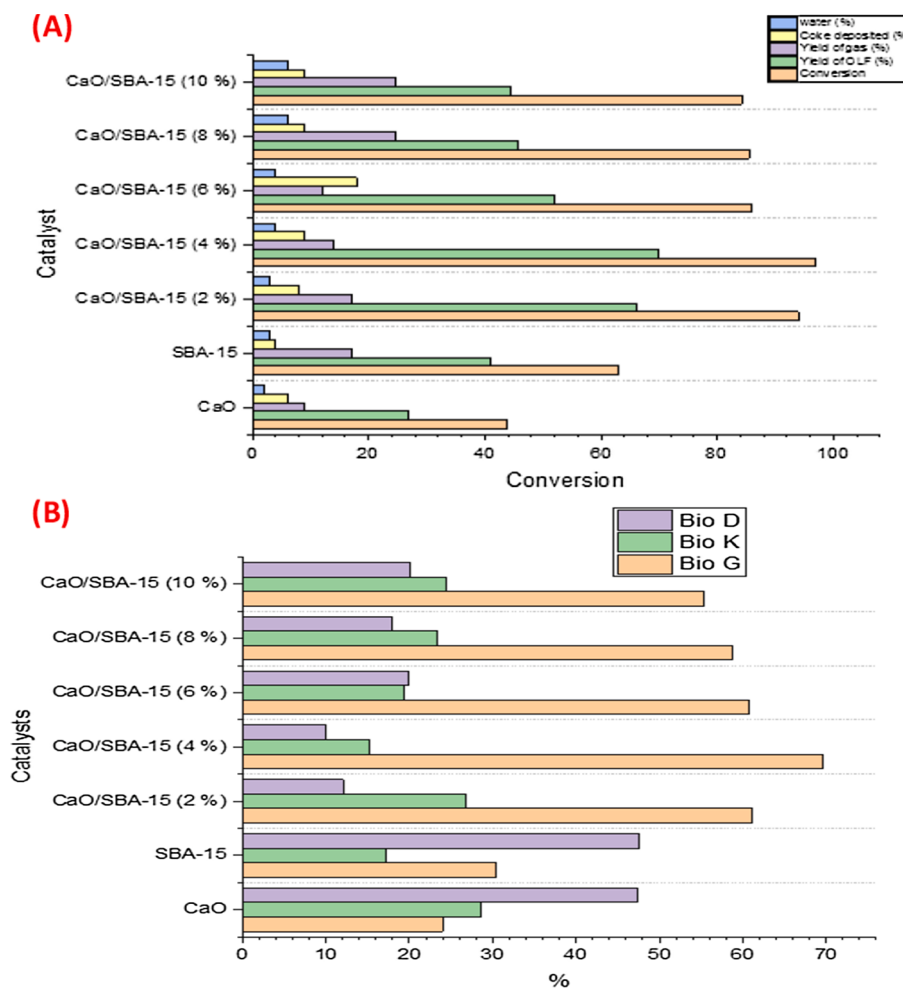


Fig. 5. a) Product distribution and b) product selectivity from catalytic cracking of UCO using CaO/SBA-15 (4 wt%).

3.2.2. FTIR spectrum analysis of BioG obtained through catalytic cracking of UCO

BioG is expected to be constituted by short & branched chain hydrocarbons and also presence of low concentrations of long range order

hydrocarbons. However, there are possibilities for the presence of oxygenated compounds which may be attributed to the meagre cracking activity of the catalyst after some duration of reaction. This may be due to the deactivation of catalyst by coke formation over the surface. The

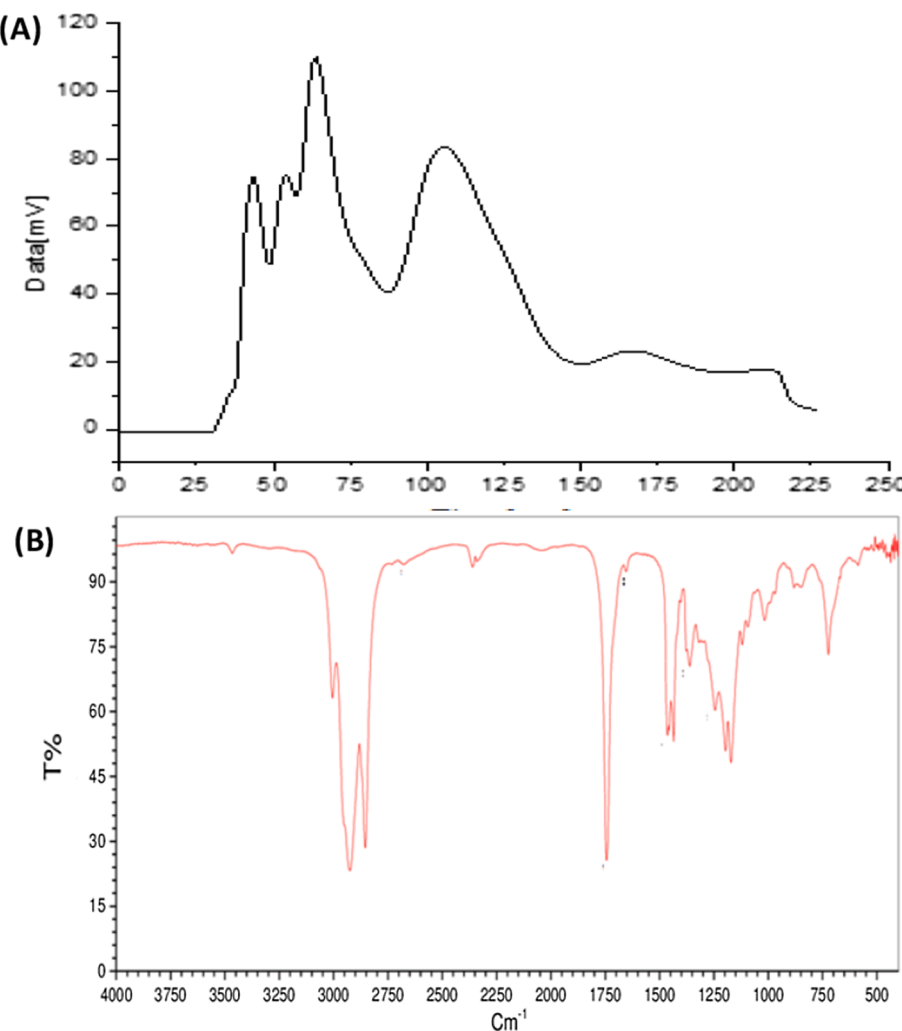


Fig. 6. a) GC MS simdistill and b) FTIR spectrum of BioG obtained from UCO.

spectrum result in Fig. 6b is in par with the expectation as it shows peaks corresponding to C–H groups and C = C groups. Alkenes gave a peak at 1640 cm^{-1} for C = C stretching vibration. Long chain saturated C–C bonds was identified by the vibration peak at 720 cm^{-1} [53]. The high intense peaks at 2900 cm^{-1} and 2800 cm^{-1} were due to the presence of methylene groups (CH_2). Although, the ester linkage of the oil is expected to be cracked, the mild cracking should be the reason for the peaks found at 1740 cm^{-1} and 1175 cm^{-1} related to C = O and C–O vibrations of ester group. The C–H groups resulted in strong vibrations at 1470 cm^{-1} . Wako et al. [54] reported a similar FTIR spectrum in their experiment of cracking waste cooking oil with a zirconium oxide catalyst. Peak was absent in the region of 3500 cm^{-1} indicating the absence of water molecules and effective cracking of oil had reduced the water molecules in BioG. It also includes the absence of water in any form ex. aliphatic and aromatic alcohol in BioG [55]. The lower intense peak at 3050 cm^{-1} confirmed the trace of aromatic compound and however, the derivatives of benzene showed peaks at 950 cm^{-1} and 800 cm^{-1} . Analogous FTIR analysis of biofuel were reported by da Silva Almeida et al. [56].

3.2.3. Properties of cracked UCO

The major physical and chemical property of BioG obtained using CaO/SBA-15 (4 %) is compared with ASTM standards of biofuel in Table 2. The table includes pour point, fire point, flash point, cloud point, specific gravity, calorific value and viscosity. The viscosity of BioG was little higher than that of fossil gasoline and which could be due

Table 2
Properties of BioG vs fossil gasoline and UCO.

Property	Unit	Method	Fossil Gasoline	UCO	BioG
Calorific value	Cal/g	ASTM D 240	10,604 to 11,297	8561	10,000
Fire point	°C	ASTM D 92	-53	345	<30
Flash point	°C	ASTM D 92	-43	305	<30
Pour point	°C	IS: 1448 Part 10	-40 to -60	9	<-10
Cloud point	°C	IS: 1448 Part 10	NA	24	<-10
Specific gravity@25 °C	—	ASTM D 1298	0.72 to 0.78	0.96	0.75
Viscosity @40 °C	Cst	ASTM D 445	0.5 to 0.6	45.35	1.2

to its low atomization. Imtenan et al. [57] studied the effect of nano additives on viscosity of biodiesel blends. The future work will be focussed in employing additives to decrease the viscosity and increase the prospects of the biofuel. Ibarra et al. [58] cracked waste vegetable oil over FCC/HZSM-5 catalyst and produced high viscous product compared to the feed. This may result in a drop in combustion efficiency along with carbon deposits. A nano additive to the produced fuel could improve the difficulty caused due to higher viscosity. The corrosive oxides released in combustion process poses threat to environment and the produced BioG looks advantageous over gasoline due to the trace

sulphur content of BioG. The flash points of the fuel lied in the range of commercial gasoline. Yigezu and Muthukumar, [59] also reported the flash point within the range of fossil gasoline. In terms of calorific value of the fuel, BioG shows low value which may influence the fuel power. Sheriff et al 2020 examined the ability of examined the ability of cerium oxide as additive to enhance the calorific value of the biofuel [60]. Similarly, the future work will concentrate on identifying the proper additive for good calorific value. A low heating value of liquid fuel produced by catalytic cracking of vegetable oils was stated by Zaher et al. [61]. However, their pour points are extremely low suggesting their possible use in hilly regions. Negm et al. [62] proposed the low pour point of biofuel prepared from jatropha oil using transition metal catalyst.

3.2.4. Engine studies using BioG blends with gasoline

This study emphasizes on the utilization of the BioG in the engine. In the standard operating condition, gasoline and BioG (10, 30 and 50%) blended with gasoline is evaluated with respect to engine performance and emission results. Works are done to operate the engine using blends of biodiesel/petro-diesel, biodiesel/ethanol and bioethanol/petro-diesel and observations have been published [63,64]. However, the reports on

operating the engine with Biofuel blends are scarce. The engine speed was varied from 1000 to 3000 RPM and various working parameters such as torque, BSFC, exhaust gas temperature, power and break thermal efficiency. Fig. 7a matches the torque of the engine with varying speed when operating using the following blends; BioG 100, BioG 50. G, BioG 30. G, BioG 30. G and BioG 10.G and for comparison purpose gasoline performance was also studied. A good torque value emphasizes on complete combustion of the fuel in the engine and low mechanical loss. On comparing the blends with gasoline, BioG 10.G provided highest torque of 31 Nm at 2000 rpm comparing the gasoline which contributed to second highest torque of 29.5 Nm at 2000 rpm. Hadhoum et al. [65] investigated the performance of olive oil mill waste water biofuel in engine and reported that 10% blend provided best engine performance compared to higher % blends. It was observed that all the blends had high torque value at 2000 rpm. The torque value increased with increase in engine speed till 2000 rpm and found to decrease with further increase in engine speed. It has to be noted that, the BioG 100 resulted in the least torque value, which dispenses further experiments with 100 % BioG. Gasoline engine was tested with bioethanol- bio-acetone – gasoline blends by Elfasakhany [66] and the results showed that 10 % blend had the highest torque.

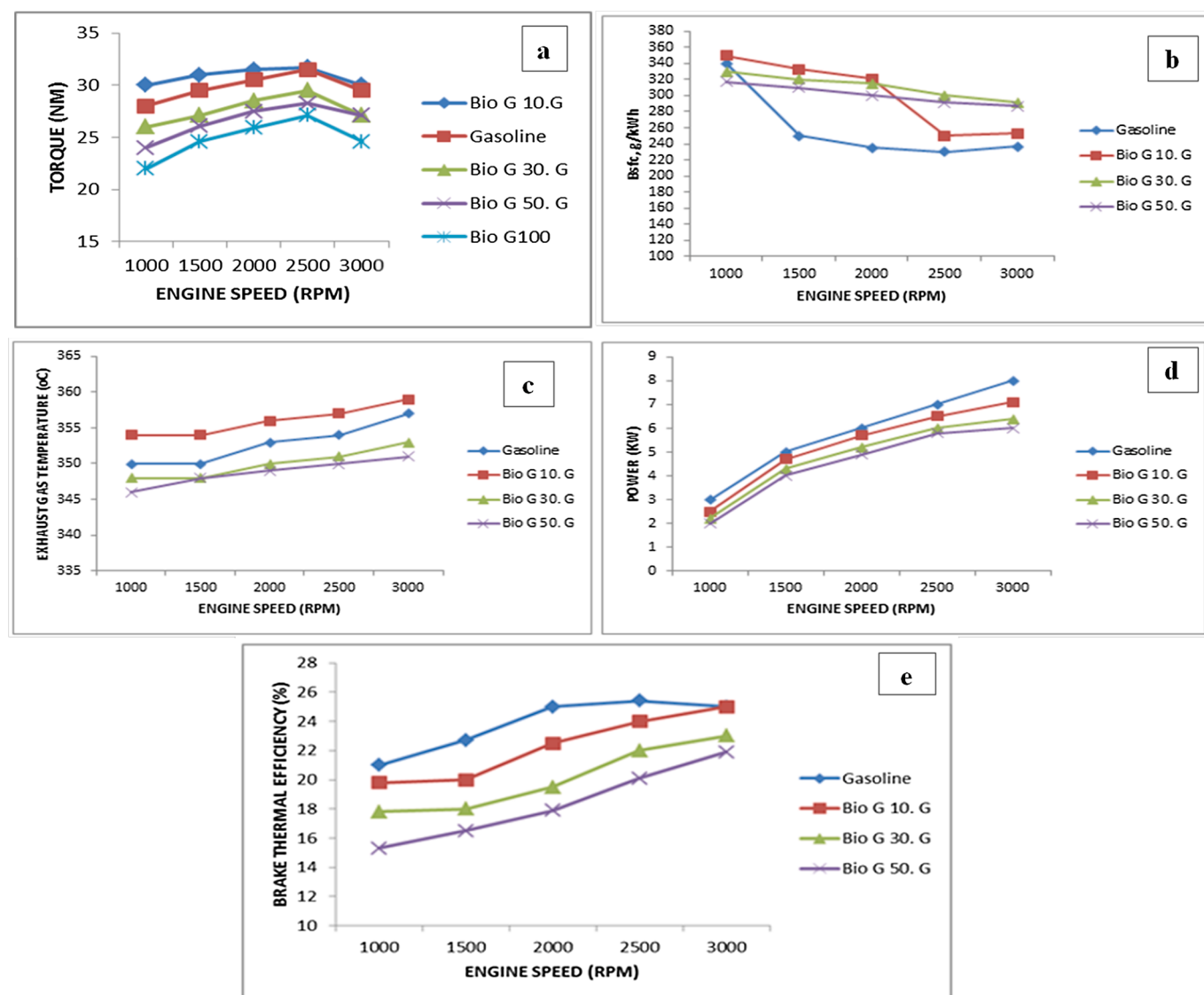


Fig. 7. Variation of a) Torque b) BSFC c) exhaust gas temperature d) power e) break thermal efficiency with different engine speeds for gasoline, BioG 10.G, BioG 30.G and BioG 50.G.

Break specific fuel consumption is calculated from rate of fuel consumption divided by power produced by the engine; hence, it is the measure of the fuel efficiency. Among the blends, BioG 10. G resulted in higher BSFC of 350 g/kwh which was even higher than the gasoline (340 g/kwh) (Fig. 7b). Catalytic pyrolysis of waste cooking oil was performed by Gad et al. [67] and examining the capacity of biofuel blends in engine showed the similar results. Whereas, a study performed by Agbulut et al. [68] witnessed a worsened trend in BSFC due to diesel/bioethanol blends. However, with increase in the engine speed, the fuel consumption of commercial gasoline decreased dramatically whereas there was a steady decrease in fuel consumption for BioG 10.G. Low BSFC of BioG 10.G can be explained by high fuel viscosity and low calorific value when compared to commercial gasoline. More biofuel is required to compensate for the decreased amount of heat released due to the reduced calorific value. When the same volume of BioG is injected, the higher density enables for more BioG to be utilised, whereas the higher viscosity impacts the volumetric fuel injection rate. The combined effect of these factors causes BioG to have a lower BSFC [69]. BioG 30.G and BioG 50.G showed less variation throughout the runs. At 3000 RPM, variation was very low; this condition may be because of the increased temperature in engine.

Exhaust gas temperature (EGT) varied with engine speed as given in Fig. 7c. EGT is an essential parameter to determine the fuel: air ratio entering the engine. Complete combustion results in higher EGT and it could be seen from the Figure that higher EGT was observed while using BioG 10. G. Ogunkunle and Ahmed, [70] analysed biodiesel blends in marine diesel engine and found 10% blend increased the EGT likewise. Gasoline and other blends have lower EGT at all the test speeds. EGT was found to increase with increase in the engine speed. As mentioned, absolute combustion of the fuel and shorter combustion duration with higher flame velocity might be the reason for the obtained results. BioG 50. G provided least EGT while comparing the gasoline and other blends. Fig. 7d illustrates the brake power generated by the engine at different engine speed starting. The engine power was seen to increase with engine speed from 1000 to 3000 RPM. Gasoline resulted in high power compared to all the blends and BioG 10.G showed good break power

among the other blends. BioG 10.G showed lower power than expected. Effect of ethanol blending with biodiesel was studied and low engine power was observed with the use of biodiesel blend compared to petro diesel [71]. This observation can be justified due to the higher values of viscosity and density of BioG.

Brake Thermal Efficiency (BTE) of an engine is defined as the brake power obtained with respect to the fuel supplied to the engine. Fig. 7e shows the comparison of BTE with varying engine speed. Maximum BTE was obtained at 2000 RPM and on with increase in engine speed, BTE decreased. Gasoline showed high BTE followed by BioG 10.G and other blends. The low BTE of the blends should be due to the low calorific value. However, at 3000 rpm, BTE was found to be same for BioG 10.5 and gasoline. This observation may be due to the complete combustion that was triggered at higher engine speed. CI engine being tested with cracked biofuel blends exhibited 36.9 % BTE in an experiment conducted by Oni et al. [72].

3.2.5. Exhaust emission analysis using BioG and the blends

Fig. 8a shows that CO emitted from BioG blends is lower than gasoline. But, there was no significant difference in CO emission at different speeds. CO emission from BioG 10.G decreased from 1000 rpm to 1500 rpm and increased further. CO emission from all the blends was low than CO emitted from gasoline combustion. The oxidation of BioG blends should be the reason for the study. The shorter duration for combustion in the engine at high engine speed should have resulted in more CO emissions. Ranjit et al. [73] proposed 0.32% of CO emission from a 4 S single cylinder engine using 30% blend of *Schleichera Oleosa* biodiesel. CO₂ emission was high for BioG 10.G compared to Gasoline fuel which emphasizes the complete combustion of BioG and also thermal efficiency has added to CO₂ emission. Edwin Geo et al. [74] reduced the CO₂ emission by using less viscous biodiesel prepared from lemon peel oil.

Fig. 8c shows the variation of Nitrous oxide for gasoline and blends of BioG at different engine speed. The NO emission was found to increase with the engine speed. NOX emission from gasoline was observed to be higher than the BioG blends at the varied engine speeds. BioG 10.G

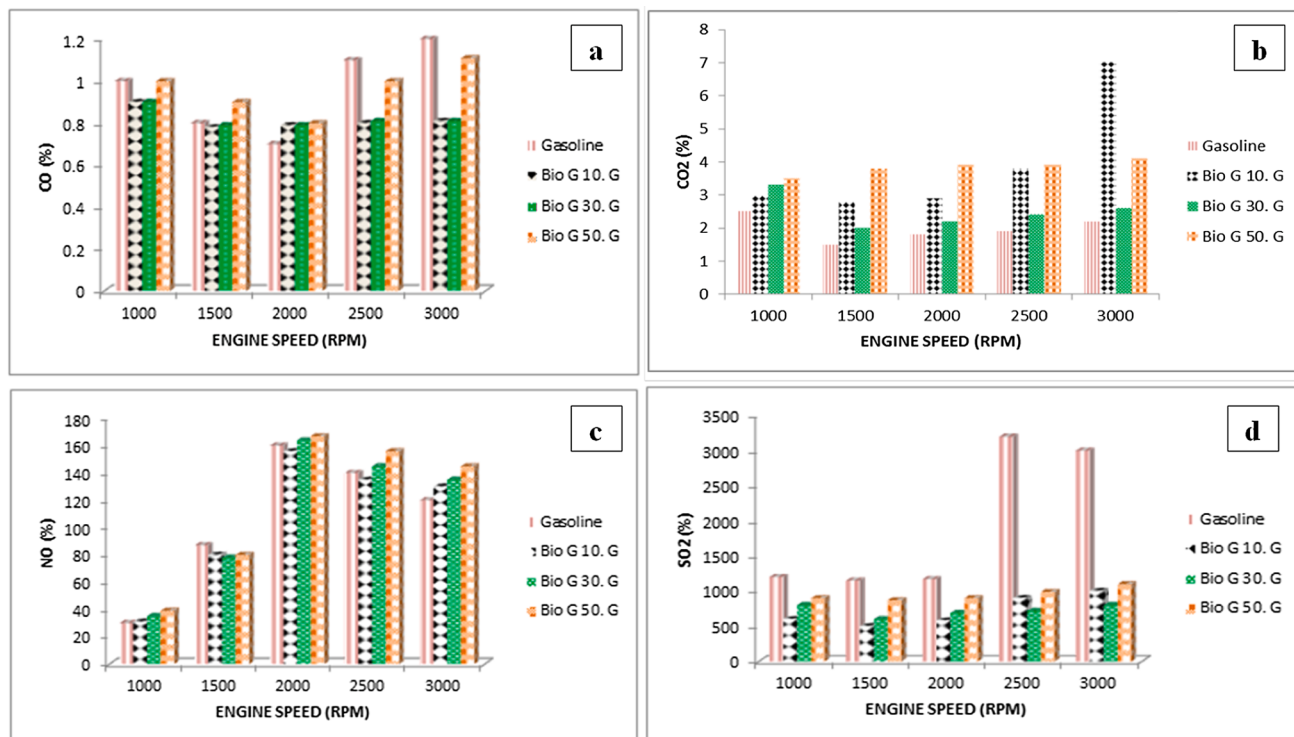


Fig. 8. Variation of a) CO b) CO₂ c) NO d) SO₂ with different engine speeds for Gasoline, BioG 10.G, BioG 30.G and BioG 50.G.

resulted in low NO emission when compared to other blends. At 1500 rpm, NO emission was low compared to rest of the engine speed. Anandhan et al. [75] used jojoba oil biodiesel blend in SI engine and observed B20 blend emitted high % of NO. Higher NO emission is determined by the complete combustion of fuel which in turn increases the temperature. Higher oxygenates in the fuel must have influenced NO_x production and also low octane index could have led to decrease of the increase in NO_x emission. Delayed ignition and fuel: air mixture accumulation is caused by low octane index which also releases heat at the start of the combustion itself. These factors induce NO_x emission..

The SO₂ emission trends for BioG blends and gasoline are shown in Fig. 8d. At low engine speeds, the SO₂ emission was low from 1000 rpm to 2000 rpm. It is convincing that, BioG blends showed low SO₂ levels compared to commercial Gasoline.

4. Conclusions

CaO/SBA-15 catalyst produced a better alternative fuel through cracking process in a fixed bed cracking unit at 450 °C. Gasoline fraction was selectively achieved in the process. Blends of BioG distilled from the liquid hydrocarbon fuel product can be used as an alternative fuel in near future without much engine modifications.

1. CaO/SBA-15 (4 wt%) converted 97 % of UCO into 70 % of liquid product with 69.7 % gasoline fraction.
2. Calorific value of 10000 MJ/Kg was attained for BioG 10.G.
3. Calorific value was found to be comparable to the conventional gasoline.
4. Better Torque was obtained in engine while using BioG 10.G compared to gasoline.
5. Power provided by BioG was bit low compared to gasoline.
6. BioG 10.G provided highest exhaust gas temperature which was higher than other blending ratios.
7. BSFC value of BioG 10.G was higher than commercial gasoline.
8. Low SO₂ emission suggests the less toxic nature of the fuel.

CRediT authorship contribution statement

Shengbo Ge: Conceptualization, Methodology, Writing - original draft. **Ramya Ganesan:** Investigation, Writing - original draft. **Manigandan Sekar:** Writing - original draft. **Changlei Xia:** Writing - review & editing, Supervision. **Shannugam Sabarathinam:** Writing - review & editing. **Mishal Alsehli:** Funding acquisition. **Kathirvel Brindhadevi:** Supervision, Project administration.

Declaration of Competing Interest

The authors declare that they have no known competing financial interests or personal relationships that could have appeared to influence the work reported in this paper.

Acknowledgements

This work was supported by Taif University researchers supporting project number (TURSP-2020/205), Taif University, Taif, Saudi Arabia. Drs. Xia and Ge thank to the funding support from Natural Science Foundation of Jiangsu Province (BK20200775), the China Postdoctoral Science Foundation (2021M690847), and the help from Advanced Analysis and Test Center of Nanjing Forestry University.

References

- [1] Zhen X, Wang Y, Liu D. Bio-butanol as a new generation of clean alternative fuel for SI (spark ignition) and CI (compression ignition) engines. *Renew Energy* 2020;147: 2494–521. <https://doi.org/10.1016/j.renene.2019.10.119>.
- [2] Edelenbosch OY, van Vuuren DP, Bertram C, Carrara S, Emmerling J, Daly H, et al. Transport fuel demand responses to fuel price and income projections: Comparison of integrated assessment models. *Transport Res Part D* 2017;55:310–21. <https://doi.org/10.1016/j.trd.2017.03.005>.
- [3] Saravanan AP, Mathimani T, Deviram G, Rajendran K, Pugazhendhi A. Biofuel policy in India: a review of policy barriers in sustainable marketing of biofuel. *J Cleaner Prod* 2018;193:734–47. <https://doi.org/10.1016/j.jclepro.2018.05.033>.
- [4] Alalwan HA, Alminshid AH, Aljaafari HAS. Promising evolution of biofuel generations. Subject review. *Renewable Energy Focus* 2019;28:127–39. <https://doi.org/10.1016/j.ref.2018.12.006>.
- [5] Callegari A, Bolognesi S, Cecconet D, Capodaglio AG. Production technologies, current role, and future prospects of biofuels feedstocks: A state-of-the-art review. *Crit Rev Environ Sci Technol* 2020;50(4):384–436. <https://doi.org/10.1080/10643389.2019.1629801>.
- [6] Ma Y, Tan W, Wang J, Xu J, Wang K, Jiang J. Liquefaction of bamboo biomass and production of three fractions containing aromatic compounds. *J Bioresour Bioprod* 2020;5(2):114–23. <https://doi.org/10.1016/j.jobab.2020.04.005>.
- [7] Foteinis S, Chatzisymeon E, Litinas A, Tsoutsos T. Used-cooking-oil biodiesel: Life cycle assessment and comparison with first-and third-generation biofuel. *Renew Energy* 2020;153:588–600. <https://doi.org/10.1016/j.renene.2020.02.022>.
- [8] Tan YH, Abdulla MO, Kansedo J, Mubarak NM, Chan YS, Nolasco-Hipolito C. Biodiesel production from used cooking oil using green solid catalyst derived from calcined fusion waste chicken and fish bones. *Renew Energy* 2019;139:696–706. <https://doi.org/10.1016/j.renene.2019.02.110>.
- [9] Alaei S, Haghghi M, Rahmaniwalid B, Shokrani R, Naghavi H. Conventional vs. hybrid methods for dispersion of MgO over magnetic Mg–Fe mixed oxides nanocatalyst in biofuel production from vegetable oil. *Renew Energy* 2020;154: 1188–203. <https://doi.org/10.1016/j.renene.2020.03.039>.
- [10] El Khatib SA, Hanafi SA, Barakat Y, Al-Amrousi EF. Hydrotreating rice bran oil for biofuel production. *Egypt J Pet* 2018;27(4):1325–31. <https://doi.org/10.1016/j.ejpe.2018.08.003>.
- [11] Shanmugam S, Hari A, Pandey A, Mathimani T, Felix LewisOscar, Pugazhendhi A. Comprehensive review on the application of inorganic and organic nanoparticles for enhancing biohydrogen production. *Fuel* 2020;270:117453. <https://doi.org/10.1016/j.fuel.2020.117453>.
- [12] Haron R, Mat R, Tuan Abdullah TA, Rahman RA. Overview on utilization of biodiesel by-product for biohydrogen production. *J Cleaner Prod* 2018;172: 314–24. <https://doi.org/10.1016/j.jclepro.2017.10.160>.
- [13] Su M, Li W, Ma Q, Zhu B. Production of jet fuel intermediates from biomass platform compounds via aldol condensation reaction over iron-modified MCM-41 lewis acid zeolite. *J Bioresour Bioprod* 2020;5(4):256–65. <https://doi.org/10.1016/j.jobab.2020.10.004>.
- [14] Zhang Y, Cui Y, Liu S, Fan L, Zhou N, Peng P, et al. Fast microwave-assisted pyrolysis of wastes for biofuels production—A review. *Bioresour Technol* 2020;297: 122480. <https://doi.org/10.1016/j.biortech.2019.122480>.
- [15] Ahmed N, Zeeshan M, Iqbal N, Farooq MZ, Shah SA. Investigation on bio-oil yield and quality with scrap tire addition in sugarcane bagasse pyrolysis. *J Cleaner Prod* 2018;196:927–34. <https://doi.org/10.1016/j.jclepro.2018.06.142>.
- [16] Fu P, Bai X, Yi W, Li Z, Li Y, Wang L. Assessment on performance, combustion and emission characteristics of diesel engine fuelled with corn stalk pyrolysis bio-oil/diesel emulsions with Ce0.7Zr0.3O2 nanoadditive. *Fuel Process Technol* 2017;167: 474–83. <https://doi.org/10.1016/j.fuproc.2017.07.032>.
- [17] Midhun Prasad K, Murugavel S. Experimental investigation and kinetics of tomato peel pyrolysis: performance, combustion and emission characteristics of bio-oil blends in diesel engine. *J Cleaner Prod* 2020;254:120115. <https://doi.org/10.1016/j.jclepro.2020.120115>.
- [18] Akah A. Application of rare earths in fluid catalytic cracking: A review. *J Rare Earths* 2017;35(10):941–56. [https://doi.org/10.1016/S1002-0721\(17\)60998-0](https://doi.org/10.1016/S1002-0721(17)60998-0).
- [19] Clough M, Pope JC, Xin Lin LT, Komvokis V, Pan SS, Yilmaz B. Nanoporous materials forge a path forward to enable sustainable growth: Technology advancements in fluid catalytic cracking. *Microporous Mesoporous Mater* 2017; 254:45–58. <https://doi.org/10.1016/j.micromeso.2017.03.063>.
- [20] Zhang J, Wu Z, Li X, Zhang Yu, Bao Z, Bai L, et al. Catalytic Cracking of Inedible Oils for the Production of Drop-In Biofuels over a SO42-/TiO2-ZrO2 Catalyst. *Energy Fuels* 2020;34(11):14204–14. <https://doi.org/10.1021/acs.energyfuels.0c02204>.
- [21] Ganesan R, Subramanian S, Paramasivam R, Sabir JSM, Femilda Josephin JS, Brindhadevi K, et al. A study on biofuel produced by catalytic cracking of mustard and castor oil using porous H β and AlMCM-41 catalysts. *Sci Total Environ* 2021; 757:143781. <https://doi.org/10.1016/j.scitotenv.2020.143781>.
- [22] Rabie AM, Mohammed EA, Negm NA. Feasibility of modified bentonite as acidic heterogeneous catalyst in low temperature catalytic cracking process of biofuel production from nonedible vegetable oils. *J Mol Liq* 2018;254:260–6. <https://doi.org/10.1016/j.molliq.2018.01.110>.
- [23] Ganesan R, Narasimhalu P, Joseph AIJ, Pugazhendhi A. Synthesis of silver nanoparticle from X-ray film and its application in production of biofuel from jatropha oil. *Int J Energy Res* 2020. <https://doi.org/10.1002/er.6106>.
- [24] Wang Y, Cao Y, Li J. Preparation of biofuels with waste cooking oil by fluid catalytic cracking: The effect of catalyst performance on the products. *Renew Energy* 2018;124:34–9. <https://doi.org/10.1016/j.renene.2017.08.084>.
- [25] Shirasaki Y, Nasu H, Hashimoto T, Ishihara A. Effects of types of zeolite and oxide and preparation methods on dehydrocyclization-cracking of soybean oil using hierarchical zeolite-oxide composite-supported Pt/NiMo sulfided catalysts. *Fuel Process Technol* 2019;194:106109. <https://doi.org/10.1016/j.fuproc.2019.05.032>.
- [26] Zheng Z, Wang J, Wei Yi, Liu X, Yu F, Ji J. Effect of La-Fe/Si-MCM-41 catalysts and CaO additive on catalytic cracking of soybean oil for biofuel with low aromatics. *J Anal Appl Pyrol* 2019;143:104693. <https://doi.org/10.1016/j.jaap.2019.104693>.

- [27] Kouzu M, Fujimori A, Suzuki T, Koshi K, Moriyasu H. Industrial feasibility of powdery CaO catalyst for production of biodiesel. *Fuel Process Technol* 2017;165: 94–101. <https://doi.org/10.1016/j.fuproc.2017.05.014>.
- [28] Zhao W, Ding H, Zhu J, Liu X, Xu Q, Yin D. Esterification of levulinic acid into n-butyl levulinate catalyzed by sulfonic acid-functionalized lignin-montmorillonite complex. *J Bioresour Bioprod* 2020;5(4):291–9. <https://doi.org/10.1016/j.jobab.2020.10.008>.
- [29] Pradana YS, Daniyanto, Hartono M, Prasakti L, Budiman A. Effect of calcium and magnesium catalyst on pyrolysis kinetic of Indonesian sugarcane bagasse for biofuel production. *Energy Procedia* 2019;158:431–9. <https://doi.org/10.1016/j.egypro.2019.01.128>.
- [30] Gan DKW, Loy ACM, Chin BLF, Yusup S, Unrean P, Rianawati E, et al. Kinetics and thermodynamic analysis in one-pot pyrolysis of rice hull using renewable calcium oxide based catalysts. *Bioresour Technol* 2018;265:180–90. <https://doi.org/10.1016/j.biortech.2018.06.003>.
- [31] Lu Q, Li W, Zhang Xu, Liu Z, Cao Q, Xie X, et al. Experimental study on catalytic pyrolysis of biomass over a Ni/Cu-promoted Fe catalyst. *Fuel* 2020;263:116690. <https://doi.org/10.1016/j.fuel.2019.116690>.
- [32] Ding K, Zhong Z, Wang J, Zhang Bo, Fan L, Liu S, et al. Improving hydrocarbon yield from catalytic fast co-pyrolysis of hemicellulose and plastic in the dual-catalyst bed of CaO and HZSM-5. *Bioresour Technol* 2018;261:86–92. <https://doi.org/10.1016/j.biortech.2018.03.138>.
- [33] Li C, Ma J, Xiao Z, Hector SB, Liu R, Zuo S, et al. Catalytic cracking of Swida wilsoniana oil for hydrocarbon biofuel over Cu-modified ZSM-5 zeolite. *Fuel* 2018; 218:59–66. <https://doi.org/10.1016/j.fuel.2018.01.026>.
- [34] Ramesh A, Tamizhdurai P, Santhana Krishnan P, Kumar Ponnusamy V, Sakthiyanthan S, Shanthi K. Catalytic transformation of non-edible oils to biofuels through hydrodeoxygenation using Mo-Ni/mesoporous alumina-silica catalysts. *Fuel* 2020;262:116494. <https://doi.org/10.1016/j.fuel.2019.116494>.
- [35] Cao X, Li Lu, Shitao Yu, Liu S, Hailong Yu, Qiong Wu, et al. Catalytic conversion of waste cooking oils for the production of liquid hydrocarbon biofuels using in-situ coating metal oxide on SBA-15 as heterogeneous catalyst. *J Anal Appl Pyrol* 2019; 138:137–44. <https://doi.org/10.1016/j.jaatp.2018.12.017>.
- [36] Zhang Y, Zhao W, Li B, Xie G. Microwave-assisted pyrolysis of biomass for bio-oil production: a review of the operation parameters. *J Energy Res Technol* 2018;140 (4). <https://doi.org/10.1115/1.4039604>.
- [37] Xu G, Jia C, Shi Z, Liang R, Wu C, Liu Hu, et al. Enhanced catalytic conversion of camelina oil to hydrocarbon fuels over Ni-MCM-41 catalysts. *Sci Adv Mater* 2020; 12(2):304–11. <https://doi.org/10.1166/sam.2020.3714>.
- [38] Mangesh VL, Padmanabhan S, Tamizhdurai P, Narayanan S, Ramesh A. Combustion and emission analysis of hydrogenated waste polypropylene pyrolysis oil blended with diesel. *J Hazard Mater* 2020;386:121453. <https://doi.org/10.1016/j.jhazmat.2019.121453>.
- [39] Ashour MK, Eldrainy YA, Elwardany AE. Effect of cracked naphtha/biodiesel/diesel blends on performance, combustion and emissions characteristics of compression ignition engine. *Energy* 2020;192:116590. <https://doi.org/10.1016/j.energy.2019.116590>.
- [40] Dinesha P, Kumar S, Rosen MA. Performance and emission analysis of a domestic wick stove using biofuel feedstock derived from waste cooking oil and sesame oil. *Renew Energy* 2019;136:342–51. <https://doi.org/10.1016/j.renene.2018.12.118>.
- [41] Esperanza Adrover M, Pedernera M, Bonne M, Lebeau B, Bucalá V, Gallo L. Synthesis and characterization of mesoporous SBA-15 and SBA-16 as carriers to improve albendazole dissolution rate. *Saudi Pharm J* 2020;28(1):15–24. <https://doi.org/10.1016/j.jpsp.2019.11.002>.
- [42] Ganeshan R, Thiruprathagan S, Subba S. Synthesis and Characterization of Core-Shell Modeled AlMCM-48/HZSM-5 Composite Catalyst and Studies on Its Catalytic Activity in Cracking of Pongamia Oil into Bio Liquid Products. *Bioenergy Res* 2019; 12(2):388–99. <https://doi.org/10.1007/s12155-019-09976-7>.
- [43] Dehghani S, Haghighi M. Sono-enhanced dispersion of CaO over Zr-Doped MCM-41 bifunctional nanocatalyst with various Si/Zr ratios for conversion of waste cooking oil to biodiesel. *Renew Energy* 2020;153:801–12. <https://doi.org/10.1016/j.renene.2020.02.023>.
- [44] Shi Z, Wu C, Wu Y, Liu H, Xu G, Deng J, et al. Optimization of epoxypipane synthesis by silicotungstic acid supported on SBA-15 catalyst using response surface methodology. *Sci Adv Mater* 2019;11(5):699–707. <https://doi.org/10.1166/sam.2019.3473>.
- [45] Li Lu, Yan B, Li H, Yu S, Ge X. Decreasing the acid value of pyrolysis oil via esterification using ZrO₂/SBA-15 as a solid acid catalyst. *Renew Energy* 2020;146: 643–50. <https://doi.org/10.1016/j.renene.2019.07.015>.
- [46] Bedoya JC, Valdez R, Cota L, Alvarez-Amparán MA, Olivas A. Performance of Al-MCM-41 nanospheres as catalysts for dimethyl ether production. *Catal Today* 2021. <https://doi.org/10.1016/j.cattod.2021.01.010>.
- [47] Khanh Nguyen QN, Yen NT, Hau ND, Tran HL. Synthesis and characterization of mesoporous silica SBA-15 and ZnO/SBA-15 photocatalytic materials from the ash of brickyards. *J Chem* 2020;2020:1–8. <https://doi.org/10.1155/2020/8456194>.
- [48] Verma P, Kuwahara Y, Mori K, Raja R, Yamashita H. Functionalized mesoporous SBA-15 silica: recent trends and catalytic applications. *Nanoscale* 2020;12(21): 11333–63. <https://doi.org/10.1039/DONR00732C>.
- [49] Thahir R, Wahab AW, La Nafie N, Rayya I. Synthesis of high surface area mesoporous silica SBA-15 by adjusting hydrothermal treatment time and the amount of polyvinyl alcohol. *Open Chem* 2019;17(1):963–71. <https://doi.org/10.1515/chem-2019-0106>.
- [50] de Sousa Castro K, Fernando de Medeiros Costa L, Fernandes VJ, de Oliveira Lima R, Mabel de Morais Araújo A, Sousa de Sant'Anna MC, et al. Catalytic pyrolysis (Ni/Al-MCM-41) of palm (*Elaeis guineensis*) oil to obtain renewable hydrocarbons. *RSC Adv* 2021;11(1):555–64. <https://doi.org/10.1039/DORA06122K>.
- [51] Mancio AA, da Costa KMB, Ferreira CC, Santos MC, Lhamas DEL, da Mota SAP, et al. Thermal catalytic cracking of crude palm oil at pilot scale: Effect of the percentage of Na₂CO₃ on the quality of biofuels. *Ind Crops Prod* 2016;91:32–43. <https://doi.org/10.1016/j.indcrop.2016.06.033>.
- [52] Micuș NJ, McCurry JD, Seeley JV. Analysis of aromatic compounds in gasoline with flow-switching comprehensive two-dimensional gas chromatography. *J Chromatogr A* 2005;1086(1–2):115–21. <https://doi.org/10.1016/j.chroma.2005.06.015>.
- [53] García-Dávila J, Ocaranza-Sánchez E, Sánchez C, Martínez-Ayala AL. Catalytic activity of a bifunctional catalyst for hydrotreatment of *Jatropha curcas* L. seed oil. *Journal of Spectroscopy* 2018;2018:5326456. <https://doi.org/10.1155/2018/5326456>.
- [54] Wako FM, Reshad AS, Bhalerao MS, Goud VV. Catalytic cracking of waste cooking oil for biofuel production using zirconium oxide catalyst. *Ind Crops Prod* 2018;118: 282–9. <https://doi.org/10.1016/j.indcrop.2018.03.057>.
- [55] Veses A, López JM, García T, Callén MS. Prediction of elemental composition, water content and heating value of upgraded biofuel from the catalytic cracking of pyrolysis bio-oil vapors by infrared spectroscopy and partial least square regression models. *J Anal Appl Pyrol* 2018;132:102–10. <https://doi.org/10.1016/j.jaatp.2018.03.010>.
- [56] da Silva Almeida H, Corrêa OA, Eid JG, Ribeiro HJ, de Castro DAR, Pereira MS, et al. Production of biofuels by thermal catalytic cracking of scum from grease traps in pilot scale. *J Anal Appl Pyrol* 2016;118:20–33. <https://doi.org/10.1016/j.jaatp.2015.12.019>.
- [57] Imtenan S, Masjuki HH, Varman M, Kalam MA, Arbab MI, Sajjad H, et al. Impact of oxygenated additives to palm and jatropha biodiesel blends in the context of performance and emissions characteristics of a light-duty diesel engine. *Energy Convers Manage* 2014;83:149–58. <https://doi.org/10.1016/j.enconman.2014.03.052>.
- [58] Ibarra Á, Hita I, Arandés JM, Bilbao J. A hybrid FCC/HZSM-5 catalyst for the catalytic cracking of a VGO/bio-oil blend in FCC conditions. *Catalysts* 2020;10(10): 1157. <https://doi.org/10.3390/catal10101157>.
- [59] Yigezu ZD, Muthukumar K. Catalytic cracking of vegetable oil with metal oxides for biofuel production. *Energy Convers Manage* 2014;84:326–33. <https://doi.org/10.1016/j.enconman.2014.03.084>.
- [60] Sheriff SA, Kumar IK, Mandhatha PS, Jambal SS, Sellappan R, Ashok B, et al. Emission reduction in CI engine using biofuel reformulation strategies through nano additives for atmospheric air quality improvement. *Renew Energy* 2020;147: 2295–308. <https://doi.org/10.1016/j.renene.2019.10.041>.
- [61] Zaher F, Gad M, Aly SM, Hamed S, Abo-Elwafa GA, Zahran H. Catalytic cracking of vegetable oils for producing biofuel. *Egypt J Chem* 2017;60(2):291–300. <https://doi.org/10.21608/ejchem.2017.2967>.
- [62] Negm NA, Zahran MK, Abd Elshafy MR, Aiad IA. Transformation of *Jatropha* oil to biofuel using transition metal salts as heterogeneous catalysts. *J Mol Liq* 2018;256: 16–21. <https://doi.org/10.1016/j.moliq.2018.02.022>.
- [63] Hassan Pour A, Safiuddin Ardebili SM, Sheikhdaoodi MJ. Multi-objective optimization of diesel engine performance and emissions fueled with diesel-biodiesel-fuel oil blends using response surface method. *Environ Sci Pollut Res* 2018;25(35):35429–39. <https://doi.org/10.1007/s11356-018-3459-z>.
- [64] Shirneshan A, Bagherzadeh SA, Najafi G, Mamat R, Mazlan M. Optimization and investigation the effects of using biodiesel-ethanol blends on the performance and emission characteristics of a diesel engine by genetic algorithm. *Fuel* 2021;289: 119753. <https://doi.org/10.1016/j.fuel.2020.119753>.
- [65] Hadhoum L, Zohra Aklouche F, Loubar K, Tazerout M. Experimental investigation of performance, emission and combustion characteristics of olive mill wastewater biofuel blends fuelled CI engine. *Fuel* 2021;291:120199. <https://doi.org/10.1016/j.fuel.2021.120199>.
- [66] Elfasakhany A. Gasoline engine fueled with bioethanol-bio-acetone-gasoline blends: Performance and emissions exploration. *Fuel* 2020;274:117825. <https://doi.org/10.1016/j.fuel.2020.117825>.
- [67] Gad MS, Abu-Elyazeed OS, Mohamed MA, Hashim AM. Effect of oil blends derived from catalytic pyrolysis of waste cooking oil on diesel engine performance, emissions and combustion characteristics. *Energy* 2021;223:120019. <https://doi.org/10.1016/j.energy.2021.120019>.
- [68] Ağbulut Ü, Polat F, Saridemir S. A comprehensive study on the influences of different types of nano-sized particles usage in diesel-bioethanol blends on combustion, performance, and environmental aspects. *Energy* 2021;229:120548. <https://doi.org/10.1016/j.energy.2021.120548>.
- [69] Wu G, Ge JC, Choi NJ. A comprehensive review of the application characteristics of biodiesel blends in diesel engines. *Appl Sci-Basel* 2020;10(22):8015. <https://doi.org/10.3390/app10228015>.
- [70] Ogunkunle O, Ahmed NA. Exhaust emissions and engine performance analysis of a marine diesel engine fuelled with Parinari polyantha biodiesel-diesel blends. *Energy Rep* 2020;6:2999–3007. <https://doi.org/10.1016/j.egyr.2020.10.070>.
- [71] Aydin H, İlkılıç C. Effect of ethanol blending with biodiesel on engine performance and exhaust emissions in a CI engine. *Appl Therm Eng* 2010;30(10):1199–204. <https://doi.org/10.1016/j.applthermaleng.2010.01.037>.
- [72] Oni BA, Sanni SE, Olabode OS. Production of fuel-blends from waste tyre and plastic by catalytic and integrated pyrolysis for use in compression ignition (CI) engines. *Fuel* 2021;297:120801. <https://doi.org/10.1016/j.fuel.2021.120801>.
- [73] Ranjit PS, Bhurat SS, Saravanan A, Murugan M, Kamesh VV, Kumar P, et al. Use of *Schleicher Oleosa* biodiesel blends with conventional diesel in a compression

- ignition engine—A feasibility assessment. Mater Today Proc 2021. <https://doi.org/10.1016/j.matpr.2021.02.370>.
- [74] EdwinGeo V, Fol G, Aloui F, Thiagarajan S, Jerome Stanley M, Sonthalia A, et al. Experimental analysis to reduce CO₂ and other emissions of CRDI CI engine using low viscous biofuels. Fuel 2021;283:118829. <https://doi.org/10.1016/j.fuel.2020.118829>.
- [75] Anandhan R, Karpagarajan S, Kannan P, Neducheralathan E, Arunprasad J, Sugumar S. Performance and emission analysis on diesel engine fueled with blends of jojoba biodiesel. Mater Today Proc 2021. <https://doi.org/10.1016/j.matpr.2021.02.165>.